Synthesis

Plant-Pollinator Specialization: Origin and Measurement of Curvature

Mannfred M. A. Boehm,[1,2,*] Jill E. Jankowski,[2,3] and Quentin C. B. Cronk[1,2]

1. Department of Botany, University of British Columbia, 3156-6270 University Boulevard, Vancouver, British Columbia V6T 1Z4, Canada; 2. Biodiversity Research Centre, University of British Columbia, 2212 Main Mall, Vancouver, British Columbia V6T 1Z4, Canada; 3. Department of Zoology, University of British Columbia, 4200-6270 University Boulevard, Vancouver, British Columbia V6T 1Z4, Canada

Submitted February 3, 2021; Accepted September 21, 2021; Electronically published December 8, 2021

Online enhancements: supplemental PDF. *Dryad data:* https://doi.org/10.5061/dryad.g1jwstqrr.

abstract: A feature of biodiversity is the abundance of curves displayed by organs and organisms. Curvature is a widespread, convergent trait that has important ecological and evolutionary implications. In pollination ecology, the curvature of flowers and pollinator mouthparts (e.g., hummingbird bills) along the dorsiventral plane has been associated with specialization, competition, and species coexistence. Six differing methods have historically been used to measure curvature in pollination systems; we provide a solution to this inconsistency by defining curvature using well-established concepts from differential geometry. Intuitively, curvature is the degree to which a line is not straight, but more formally it is the rate at which the tangent of a curve changes direction with respect to arc length. Here, we establish a protocol wherein a line is fitted against landmarks placed on an image of a curved organ or organism, then curvature is computed at many points along the fitted line and the sum taken. The protocol is demonstrated by studying the development of nectar spur curvature in the flowering plant genus *Epimedium* (Berberidaceae). By clarifying the definition of curvature, our aim is to make the language of comparative morphology more precise and broadly applicable to capture other curved structures in nature.

Keywords: curvature, floral diversity, hummingbird, measure, morphometrics, pollination.

> We are beginning to understand why some hummingbird bills are long, whereas others are short, and why some hummingbird flowers are wide, whereas others are narrow. Now, why are bills of some hummingbirds and the tubes of the flowers they visit curved? (Temeles 1996)

* Corresponding author; email: mannfred.boehm@ubc.ca.

ORCIDs: Boehm, https://orcid.org/0000-0002-2537-3490; Jankowski, https://orcid.org/0000-0003-3273-1388; Cronk, https://orcid/0000-0002-4027-7368.

The Ecology of Flower-Pollinator Curvature

At the center of plant-pollinator diversification is a remarkable variety of floral form. The notion that plant communities experience selection to reduce interspecific mating ("floral isolation"; Grant 1949) points to the importance of floral diversity in initiating and reinforcing reproductive isolation (Armbruster and Muchhala 2009). For example, patterns of character displacement in sympatric *Centropogon* C.Presl (Campanulaceae) suggest that competition for pollinators led to the divergence of floral traits associated with bat and hummingbird pollination (Lagomarsino and Muchhala 2019). In the case of South African *Lapeirousia* Pourr. (Iridaceae), geographic variation in floral tube length has subsequently initiated reproductive isolation between morphs with short and long corolla tubes despite sharing the same fly pollinator (Minnaar et al. 2019). While patterns of plant-pollinator evolution point to both contemporaneous and asymmetrical coadaptation (Cardinal and Danforth 2013; Tripp and McDade 2013), floral morphology can be both the cause and the result of plant-pollinator diversification (Kay and Sargent 2009; Niet and Johnson 2012; Ollerton 2017).

Flower-pollinator curvature as viewed from the side (dorsiventral plane) has been a trait of special interest throughout the post-Darwin era of pollination ecology. However, some floral curvature has origins that may precede any particular ecological function. Instead, curved flower parts (e.g., nectar spurs) might develop within buds when constrained for space. That is, during bud development nectar spurs elongate and curve when met with resistance from the enclosing bud tissue. Following bud opening, flower parts may straighten but retain some degree of curvature at maturity. While curvature may thus originate from a

  https://doi.org/10.1086/717677

developmental constraint or lack of selection for straightness, there can be positive selection for curvature when it increases the complexity of nectar extraction and mechanical interaction between the anthers and the body of the pollinator (Collins 2008; Young 2008).

One consequence of floral curvature is pollinator partitioning. In making pollinator observations of the Cape flora, Scott-Elliott (1890) noticed that the flowers of *Leonotis ocymifolia* (Burm.f.) Iwarsson (Lamiaceae) visited by sunbirds (Nectariniidae) were "curved with the same curvature as that of the bird's beak" (p. 272). Robertson (1889) insightfully noted that the curved nectar spur of *Viola* L. (Violaceae) "serves to limit the insect visits much more than the mere length of the spur" (p. 172). Stiles (1975) first posited that Neotropical *Heliconia* L. (Zingerberales) partition hummingbird (Trochilidae) visitation by flower and bill curvature and that specialization by curve-billed hummingbirds allows coexistence within this species-rich clade. Subsequent research supports this hypothesis (Maglianesi et al. 2014): along the slopes of the Central Cordillera of Costa Rica, the degree of flower and hummingbird bill curvature is proportional to plant-pollinator interaction strength (sensu Dehling et al. 2014) and extent of specialization (sensu Blüthgen et al. 2006). In addition to interspecific partitioning of resources, many hummingbirds exhibit sexual dimorphism in bill shape: females have greater bill curvature than males and forage for nectar from curved flowers (Temeles et al. 2005, 2010). Explanations for this pattern range from reduced competition for nectar resources between sexes (Paton and Collins 1989; Temeles et al. 2019) to selection for mechanically superior bill shapes during male-male competition for territories (Rico-Guevara and Araya-Salas 2014). While the examples given above have focused on downward curvature of the bill, some hummingbird species (e.g., *Ensifera ensifera*) have bills with upward curvature. These species feed from pendant (straight) flowers by approaching from the bottom (Stiles 2008), where their recurved bills might assist in pulling the flowers upright while feeding. This trait is associated with specialists of montane plant taxa with long, pendant flowers (e.g., *Fuchsia* L., *Passiflora* L.; Stiles 2008). Therefore, upward bill curvature might also evolve via selection for pollinator partitioning, where pendant flowers, and not floral curvature, restrict access to hummingbirds with recurved bills. Thus, even from the earliest observations, curvature has been synonymous with specialization; we expect curvature to limit the range of functional taxa in a plant-pollinator mutualism and strengthen interactions between the existing participants.

More recently the scope of plant-hummingbird research has expanded to address the biogeography of curvature. As predicted by Stiles (2004), Maglianesi (2015*a*) and Sonne (2019) found plant-hummingbird curvature to be more represented across species in the lowlands of the Neotropics than in higher elevations. In this case, plant-pollinator curvature is a form of niche divergence evolving in species-rich lowland habitats, where species experience relatively higher competition (e.g., for nectar or pollen vectors) than in the adjacent Andes mountains (Stiles 2004; Graham et al. 2009). Furthermore, because plant and hummingbird morphology are better matched (i.e., more specialized) at lower latitudes (Sonne et al. 2020) and hummingbirds with curved bills are predominately tropical, we might expect the occurrence of curvature in these taxa to have a predictable latitudinal distribution.

While curvature mediates specialization in plant-hummingbird systems, in other nectarivorous bird groups curvature appears to evolve in the absence of selection for resource partitioning. In plant-passerine systems, curvature is more prevalent in pollinators than in flowers. Straight flowers do not necessarily exclude pollination by curve-billed birds; for example, the straight, tubular flowers of African *Aloe* L. (Asphodelaceae) are pollinated by curve-billed sunbirds (Paton and Collins 1989), and the small campanulate flowers of *Vaccinium* L. (Ericaceae) are pollinated by the Hawaiian honeycreeper *Drepanis coccinea* (Fringillidae; Carothers 1982). For these passerine clades, a dietary shift to nectarivory may drive the evolution of bill curvature because (ancestral) insect-pollinated plants require perching at angles not directly facing the flower opening (Paton and Collins 1989). Furthermore, probing concealed nectar from a fixed perch is an inherently arc-like motion (analogous to reaching into a tall cup to extract, say, an ice cube). Recent experimental work found that Amethyst sunbirds (*Chalcomitra amethystina*) extract nectar more efficiently when flowers are curved toward a perch, indicating that bill curvature may evolve from the arc-like motion of probing tubular flowers (Johnson et al. 2020).

A comparison of honeyeaters (Meliphagidae; predominately Australasian), sunbirds (Africa, Australasia), Hawaiian honeycreepers, and hummingbirds (Nearctic, Neotropic) suggests that downward bill curvature is widespread in the passerine families, but in hummingbirds the majority of species with decurved bills occur in subfamily Phaethornithinae (Paton and Collins 1989). While hummingbirds possess unique musculature and wing shape for hovering and maneuvering adeptly while feeding (Dakin et al. 2018), passerines typically perch to probe for nectar. For plant-passerine systems, primarily insectivorous birds may have evolved curved bills to feed at awkward angles from plants with straight, tubular flowers, and only in some cases does reciprocal adaptation produce curved flowers, for example, sunbird-pollinated *Streptocarpus dunnii* Mast. (Gesneriaceae; Hughes et al. 2007). The evolution of reciprocal curvature in such plants may be driven by selection either to exclude inefficient pollinators such as bees, which otherwise

would compete for nectar and pollen, or to increase the precision of pollen placement. It is worth noting that in landbirds the evolution of bill shape is coupled with skull shape (Bright et al. 2016; Navalón et al. 2020). Therefore, for some nectarivorous passerines the evolution of bill shape is influenced not only by flower morphology but also by the biomechanical factors that restrict skull shape (Navalón et al. 2020). Thus, unlike in plant-hummingbird systems (in which curvature mediates pollinator partitioning), selection for downward curvature in plant-passerine systems appears to operate on nectarivorous birds more so than the plants they pollinate.

Floral diversity contributes to floral isolation and diversification in the angiosperms (Armbruster and Muchhala 2009; Kay and Sargent 2009; Vamosi et al. 2018). Similarly, dietary specialization within pollinator clades has contributed to the diversification of mouthpart morphology (Weinstein and Graham 2017; Maruyama et al. 2018). In both cases, curvature is a widespread feature of morphological diversity. Therefore, to synthesize our knowledge of curved plant-pollinator systems, curvature is a concept that needs an exact definition and method of measurement. In the following section, we summarize the approaches used in measuring curvature within the field of pollination ecology and evaluate the strengths and shortcomings of each. Building on this assessment, we offer a conceptualization of curvature that improves the precision of measurement of this trait. Although this review is motivated by the problem of measuring curvature in plant-pollinator systems, the solution is general to any biological form modeled as a line curve; we then apply this method to floral curvature in an example demonstration.

Summary of the Literature: History of Measuring Curvature in Pollination Ecology

We searched the scientific literature for studies of floral or pollinator mouthpart curvature, as these traits are commonly measured as a proxy for specialization. We make the distinction between measuring curvature in a single plane (e.g., the dorsiventral plane of flowers) versus the curvature of surfaces. While single-plane images are analyzed for line curvature, measurements of specimens measured in two planes (e.g., dorsiventral and transverse) can be used to analyze surface (Gaussian) curvature (Nath et al. 2003). At present, surface curvature has yet to be considered in the context of pollination. Nonetheless, line and surface curvature are related mathematical concepts, so it will benefit pollination research to clarify the simplest case (lines) with the goal of generating interest in related ideas, including the curvature of surfaces.

The literature was sourced by querying Web of Science and Google Scholar for a topic search of (curv*) AND (pollinat*) AND (flower OR corolla OR *bird OR *bee OR moth OR *fly). The initial search returned more than 300 studies that were then screened for those that measured curvature of floral organs (e.g., petals, styles) and/or animal mouthparts (e.g., bird bills, moth tongues). We sorted studies based on the criteria that (1) the study focused on petal curvature or animal pollination, including qualitative measures of curvature, or (2) the study measured curvature of a floral organ other than petals (e.g., style curvature in autogamous species) or animal mouthparts outside a pollination context (e.g., taxonomic classification). Under the first criterion, 48 studies were identified to have used some form of curvature metric (table 1). An additional 13 studies (second criterion) are included in table S1 (tables S1–S8 are available online). There were numerous studies of plant-animal morphology that did not address curvature; these were omitted from our analysis.

In our survey, the dedicated discussion of dorsiventral curvature in plant-pollinator interactions begins with Hainsworth (1973), in reference to *Heliconia* and hermit hummingbirds. Curvature in pollination ecology is first empirically studied by Gill and Wolf (1978), although methods for measuring curvature of bird appendages outside a pollination context can be found much earlier (Baldwin et al. 1931, p. 107). We identified six common approaches to measuring curvature in pollination systems. These are (1) qualitative description (e.g., "very curved," "less curved"), although this is generally no longer used; (2) the arc-to-chord method, which defines curvature as a ratio of two lines (an arc fitted to the curve of a flower or mouthpart [e.g., bird bill] from its tip to its base and the straight line [chord] subtending the arc; fig. 1); (3) the mandibular index, which defines curvature as a ratio of two lines (a straight line from base to tip [chord] and a perpendicular line that measures the maximum height of the flower/bill arc [versine]); (4) the angle of deflection method, which defines curvature as the angle between the tangent line at the base of the flower/bill and the straight line from base to tip (chord); (5) the inverse radius method, which approximates the arc of the flower/bill as a segment of a circle (curvature is defined as the inverse radius of the fitted circle); and (6) geometric morphometrics (GM), which defines and quantifies shape as a configuration of homologous points (landmarks) existing on a coordinate plane (fig. S1; figs. S1–S9 are available online).

The strength of methods 2–5 are their portability and accessibility. These measurements can be taken in the field without sensitive digital equipment (i.e., in inclement weather) or determined easily from standardized photographs. The methods are intuitive and in the simplest case require only a ruler, string, and protractor. Temeles (2009) pointed out that for curves well fitted by a circle, the inverse radius method is interchangeable with the angle of deflection method because the radius can be calculated from the

length and angle of a chord (fig. S2; Bell 1956). Similarly, for circles, arc length and versine can be computed from the radius and angle of deflection (Zwillinger 2018, pp. 424–425). Given the required additional geometric information, for curves well fitted by a circular arc, methods 2–5 will provide equivalent rank orders.

In fitting a curve with a circle, we assume that curvature is constant across the specimen. However, when curvature deviates from constant, methods 2–5 are less suitable (discussed in Berns and Adams 2010). The angle of deflection and mandibular index are computed from only two or three landmarks, respectively. Any changes in curvature between landmarks are not considered—this is problematic when curvature varies across the specimen (e.g., a hook at the end of a bird bill). The inverse radius method assumes the curve to have constant curvature. The arc-to-chord method, because it considers arc length, implicitly contains information about curvature across the entire specimen—for a curved line in a plane, arc length and total curvature are proportional (see the following section). However, the curvature of a local feature cannot be extracted given only the length of the arc and chord. Overall, while these methods succeed in estimating the total curvature of an entire curve, they are not designed to account for fluctuating curvature caused by locally curved features.

An additional problem is a lack of consensus terminology and methodology. For example, the arc-to-chord method is also called the "maxillary index," while the angle of deflection is sometimes referred to as the "angle of declension." Many studies create their own terminology for the concept of arc length: the length of a curve between two points. Most studies define their own terms for measuring and reporting curvature without reference to previous studies. We found no discussion of units or of their meaning, which creates uncertainty about how to compare and convert metrics used between studies. We also found no discussion or methods accounting for allometry. For example, the arc-to-chord method will give the same curvature values for a set of isometrically scaled curves. However, for the inverse radius method, curvature is defined by size (radius); by definition, larger specimens will have less curvature. Therefore, an analysis of shape, including curvature, needs to consider how allometry will affect the interpretation of the results (Klingenberg 2016). We believe these problems could be remedied by referring to the mathematical literature for the derivation and definition of curvature and related concepts.

Starting with Berns and Adams (2010), GM emerges in the literature addressing curvature in pollination systems. GM is a robust toolkit for testing the covariance of shape (sensu Bookstein 1991) and ecological variables, for example, how flower shape might covary with local pollinator communities (Gómez et al. 2009). This approach has steadily gained in popularity because of its mathematical rigor, reproducibility, and the appealing visual representations of shape variation (Olsen 2017). Additionally, because GM has a traceable mathematical lineage (Bookstein 1991), its vernacular is well defined and used consistently between practitioners. Here, we highlight some of the most important features of GM to introduce relevant concepts, and we recommend the concise and authoritative introduction by Webster and Sheets (2010) for more details.

In traditional morphometrics, univariate measurements (such as length, width, and angle) are the primary data used to quantify shape. Methods 2–5 fit into this category. Typically, these measurements are anchored by landmarks—topologically or biologically homologous points that can be located on all specimens (detailed in Bookstein 1991; MacLeod 1999). In geometric morphometrics, landmarks are assigned across the specimen, with the goal of representing its shape as completely as possible. A typical protocol for a 2D object begins by placing the specimens on an *xy*-grid and assigning *xy*-coordinates to landmarks (fig. S1). In a comparative study, the samples are overlaid so that their shape information is isolated from their orientation, location, and size. This is done using a least squares–type protocol, most commonly the generalized Procrustes analysis (Rohlf and Slice 1990). In outline-based GM, the *xy*-coordinates of landmarks are fitted by form or shape functions (sensu MacLeod 2012) and decomposed by elliptic (Kuhl and Giardina 1982) or ZR (Zahn and Roskies 1972) Fourier analysis, respectively. Harmonic shape variables from a Fourier analysis are then used to calculate the principal components of shape variation (MacLeod 2012). In landmark-based GM, the set of landmarks summarizing the shape of an organism is treated as a "landmark configuration." Configurations exist in a shape space defined by the number of landmarks and spatial dimensions implemented. These configurations are then projected onto a simpler Euclidean space, analogous to the reduction of a spherical Earth onto a two-dimensional map (Webster and Sheets 2010). From here, familiar statistical procedures (e.g., principal component analysis [PCA]) can be performed to quantify variation in landmark configurations (shape) between samples.

A typical presentation of a shape PCA attaches end-member specimens (MacLeod 2002) or end-member deformation grids (Bookstein 1991) at both ends of a given principal axis. This enables a qualitative description of the primary trait(s) varying along said axis. For example, visual inspection of deformation grids along PC2 of figure 2 could be interpreted as shape variation driven by differences in floral curvature. However, the limitation of landmark-based GM in the quantification of curvature is that this method is concerned with analyzing the entirety,

Table 1: Summary of literature reviewed for metrics of floral or mouthpart curvature in plant-pollinator systems

Citation	System	Stated or inferred method
Snow and Snow 1972	Bill morphology and niche partitioning of nine hummingbird species in the Arima Valley, Trinidad	Qualitative
Stiles 1975	Corolla morphology of *Heliconia* (Zingerberales) and bill morphology of nine hummingbird species at La Selva, Costa Rica	Qualitative
Feinsinger and Colwell 1978	Bill morphology and niche partitioning within hummingbird communities of the Caribbean Islands and Monteverde, Costa Rica	Qualitative
Gill and Wolf 1978	Sunbird bill diversity and abilities to extract nectar from Kenyan *Leonotis nepetifolia* (Lamiaceae)	Mandibular index
Carothers 1982	Variation in bill morphology in three species of Hawaiian honeycreepers and effects on feeding performance in *Vaccinium calycinum* (Ericaceae)	Angle of deflection
Grant and Grant 1983	Effects of Hawkmoth proboscis length on pollination of *Mirabilis longiflora* (Nyctaginaceae)	Qualitative
Stein 1987	Biogeography, evolution, and pollination of hummingbird-pollinated *Centropogon* (Lobelioidae) with curved flowers	Angle of deflection
Mountainspring 1987	Sexual dimorphism and foraging preferences of the Maui parrotbill (*Pseudonestor xanthophrys*)	Mandibular index
Paton and Collins 1989	Functional ecology of bill shape in hummingbirds, honeyeaters, sunbirds, and Hawaiian honeycreepers	Mandibular index
Muller 1995	Curved bristles on the proboscis of European bees for the extraction of pollen	Qualitative
Smith et al. 1995	Correlated evolution of diet and bill shape in Hawaiian honeycreepers	Inverse radius
Stiles 1995	Effects of bill morphology on insect foraging strategy by 11 species of hummingbirds at La Selva, Costa Rica	Arc-to-chord ratio
Mclntyre and Browne 1996	Phototropism in *Helianthus* (Asteraceae) and effects on cotyledon curvature	Angle of deflection
Manning and Goldblatt 1997	Comparative floral morphology of fly-pollinated Iridaceae, Geraniaceae, and Orchidaceae of South Africa	Qualitative
Cotton 1998	Survey and description of 16 hummingbird species occurring in Amacayacu National Park, Colombia	Qualitative
Temeles et al. 2000	Sexual dimorphism of bill shape in purple-throated caribs (*Eulampis jugularis*) and effects on pollination of *Heliconia* at Quilesse Reserve, Saint Lucia	Angle of deflection, inverse radius
Borgella et al. 2001	Effects of bill morphology (21 hummingbird species) on pollen loads (35 plant species) at Coto Brus, Costa Rica	Arc-to-chord ratio
Temeles and Kress 2003	Sexual dimorphism of bill shape in purple-throated caribs (*Eulampis jugularis*) and effects on pollination of *Heliconia* in Saint Lucia and Dominica	Angle of deflection
Travers et al. 2003	Nectar spurs of *Impatiens* species and ruby-throated hummingbirds (*Archilochus colubris*) in Franklin County, Massachusetts	Angle of deflection
Temeles et al. 2005	Sexual dimorphism of bill shape in purple-throated caribs (*Eulampis jugularis*) and effects on pollination of *Heliconia* at Quilesse Reserve, Saint Lucia	Angle of deflection, inverse radius
Collins 2008	Foraging efficiency from artificial and natural (15 species) flowers by four species of hummingbirds in Monteverde, Costa Rica	Mandibular index
Stiles 2008	Correlations of bill morphology to the elevational distributions of 150 species of hummingbirds in the Andes	Arc-to-chord ratio
Young 2008	Effects of spur shape on male and female fitness in *Impatiens capensis* (Balsaminaceae)	Angle of deflection
Martén-Rodríguez et al. 2009	Testing the pollination syndrome hypothesis in Antillean Gesneriaceae	Angle of deflection
Temeles et al. 2009	Effects of natural (*Heliconia*) and artificial flower morphologies on foraging performance of purple-throated caribs (*Eulampis jugularis*) in Saint Lucia	Angle of deflection, inverse radius
Luo and Li 2010	Effects of light and temperature on style curvature in *Alpinia* (Zingiberaceae)	Angle of deflection

Temeles et al. 2010	Sexual dimorphism of bill shape in 21 species of Central and South American hummingbirds	Angle of deflection, inverse radius
Berns and Adams 2010	Sexual dimorphism of bill shape in black-chinned hummingbirds (*Archilochus alexandri*) and ruby-throated hummingbirds (*Archilochus colubris*)	Geometric morphometrics
Berns and Adams 2013	Sexual dimorphism of bill shape in 219 hummingbird species	Geometric morphometrics
Wang et al. 2013	Selection for nectar spur curvature in *Impatiens oxyanthera* (Balsaminaceae) mediated by pollinators and nectar robbers	Angle of deflection
Maglianesi et al. 2014	Elevational variation in plant-hummingbird network structure mediated by bill morphology (La Selva, Costa Rica)	Angle of deflection
Rico-Guevara and Araya-Salas 2014	Selection for bill shape driven by male-male competition in *Phaethornis longirostris* (La Selva, Costa Rica)	Arc-to-chord ratio
Alexandre et al. 2015	Quantitative trait locus (QTL) analysis comparing hummingbird-pollinated and generalist *Rhytidophyllum* flowers (Gesneriaceae)	Angle of deflection
Campos et al. 2015	Generation of 3D-printed flowers to experimentally study the feeding mechanics of moth pollination	Curve decay parameter
Maglianesi et al. 2015*b*	Differential preferences of artificial and natural (65 species) flower populations visited by three species of hummingbirds in Braulio Carrillo National Park, Costa Rica	Angle of deflection
Maglianesi et al. 2015*a*	Plant-pollinator specialization along an elevational gradient in Braulio Carrillo National Park, Costa Rica (21 hummingbird species and 208 plant species examined)	Angle of deflection
Rocha et al. 2015	Physical and biochemical basis for androgynophore bending in bat-pollinated *Passiflora mucronata* (Passifloraceae)	Arc-to-chord ratio
Miller et al. 2017	Ecological divergence among closely related, morphologically similar honeyeaters co-occurring in arid Australian environments	Arc-to-chord ratio
Lagomarsino et al. 2017	Evolution of pollination syndromes in Andean Campanulaceae	Arc-to-chord ratio
Boehm 2018	Review of nectar robbing in *Centropogon* (Campanulaceae)	Qualitative
Hadley et al. 2018	Effects of forest fragmentation on hummingbird bill morphologies (19 species) representative of specialization (Coto Brus, Costa Rica)	Arc-to-chord ratio
Joly et al. 2018	Testing the pollination syndrome hypothesis in Antillean Gesneriaceae	Geometric morphometrics
Partida-Lara et al. 2018	Spatiotemporal structure of the taxonomic and functional diversity of hummingbirds at the biosphere reserve El Triunfo, Chiapas, Mexico	Inverse radius
Dellinger et al. 2019	Floral trait changes correlated with the repeated shifts away from buzz pollination in the Melastomataceae	Qualitative
Peng et al. 2019	Evaluation of fitness optima of the moth proboscis and flower shape	Curve decay parameter
Sonne et al. 2019	Variation strength of plant-hummingbird specialization along an elevational gradient in Podocarpus National Park, Ecuador	Arc-to-chord ratio
Johnson et al. 2020	Experimental effects of floral orientation and curvature on nectar extraction by Amethyst sunbirds (*Chalcomitra amethystina*)	Angle of deflection
Puga-Caballero et al. 2020	Cities as environmental filters acting on hummingbird bill morphology (20 species) and community structure along the Trans-Mexican Volcanic Belt	Angle of deflection

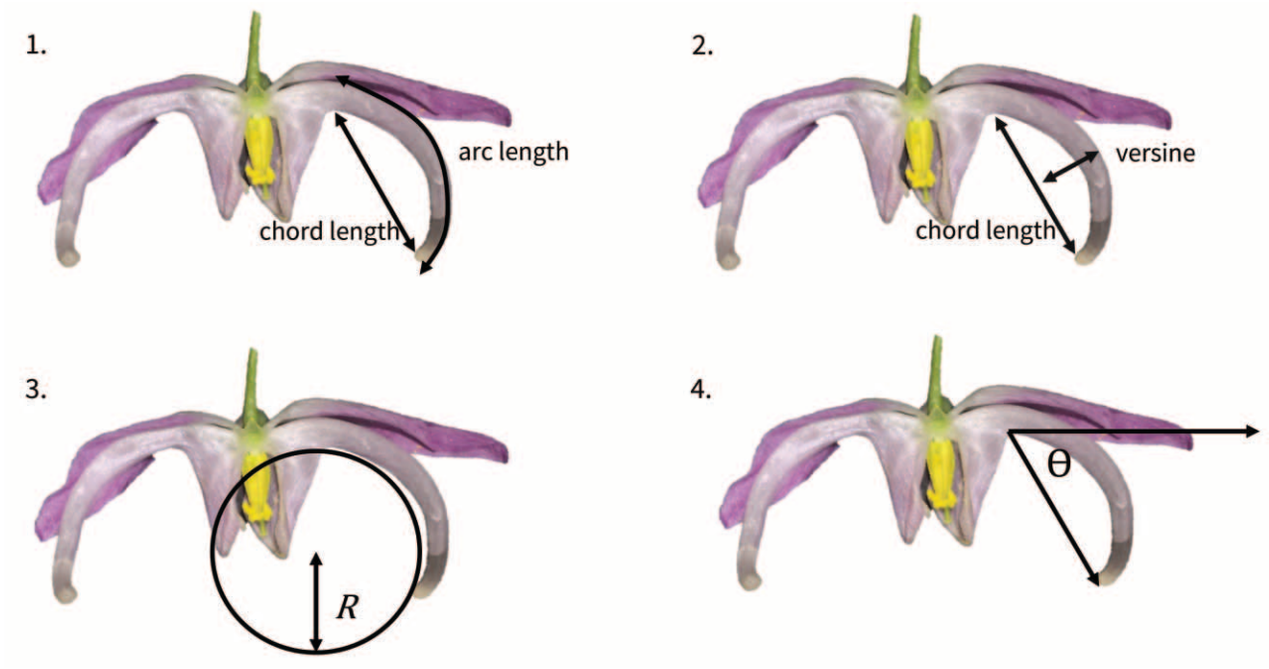

Figure 1: Overview of most commonly used curvature metrics within pollination ecology: (1) arc-to-chord ratio, (2) mandibular index, (3) inverse radius, and (4) angle of deflection.

not the segments, of a specimen's shape. Outline-based GM, though well suited to analyzing open curve segments (MacLeod 1999), lacks a method for specifically extracting information about curvature. Therefore, while GM has enabled the quantification of shape, we are currently limited to describing curvature by visual inspection of the principal axes of shape space.

Curvature: Concepts from Differential Geometry

Reviewing the literature leads us to ask, What is curvature? In related fields—for instance, in plant physiology—there have been uses of a pointwise definition of curvature resembling that used in differential geometry (Castle 1962). However, as in pollination ecology, references to the mathematical literature are missing. Therefore, we propose turning to the field of geometry in order to develop the concept of curvature starting from first principles. There, we again find several definitions resulting from a history of independent derivations (reviewed in Coolidge 1952; Bardini and Gianella 2016). Nonetheless, these definitions share a conceptual theme; curvature is a local property that can be measured pointwise on a line. This concept is fundamentally different from those typically used in pollination ecology, where curvature is a single property of an entire shape. Here, we follow the conventions of Casey (1996) and Rutter (2000) and present a definition of curvature that is tractable for analyzing biological shapes.

Intuitively, when a line deviates from being straight we say it is curved, the extent to which it is not straight is its curvature. More technically, a line deviates from being straight when its slope (i.e., the graph of the first derivative) changes magnitude—this is represented here by the rotating unit tangent vectors $\mathbf{T}_0$, $\mathbf{T}_2$, $\mathbf{T}_7$, and $\mathbf{T}_n$ in figure 3. Therefore, curvature can be thought of as the rate of change in the tangent as we move across the curve. Hence, the tangents of a straight line will have the same slope everywhere and the line will have a curvature of zero, whereas when the slopes of the tangents of a curve fluctuate, the line will have nonzero curvature.

As biological curves often loop back on themselves (e.g., spirals), they are best described by parametric functions. By using a "hidden" variable that determines the values of x and y independently, parametric functions allow a curve to have multiple y values for a single x. Here, we use the parameter variable arc length, s, along the curve, to give us the x and y position. Specifically, we can express a position vector $\mathbf{r} = [x, y]$ as a function solely of arc length, s. Using vector notation, we have

$$\mathbf{r}(s_i) = \mathbf{r}_i \equiv \begin{bmatrix} x(s_i) \\ y(s_i) \end{bmatrix}.$$

Here, $\mathbf{r}_i$ is shorthand for $\mathbf{r}(s_i)$, which indicates that our position $(x(s_i), y(s_i))$ on the curve is determined by the length of the segment s_i. Although we could parameterize a curve by many potential parametric variables, arc length is a convenient

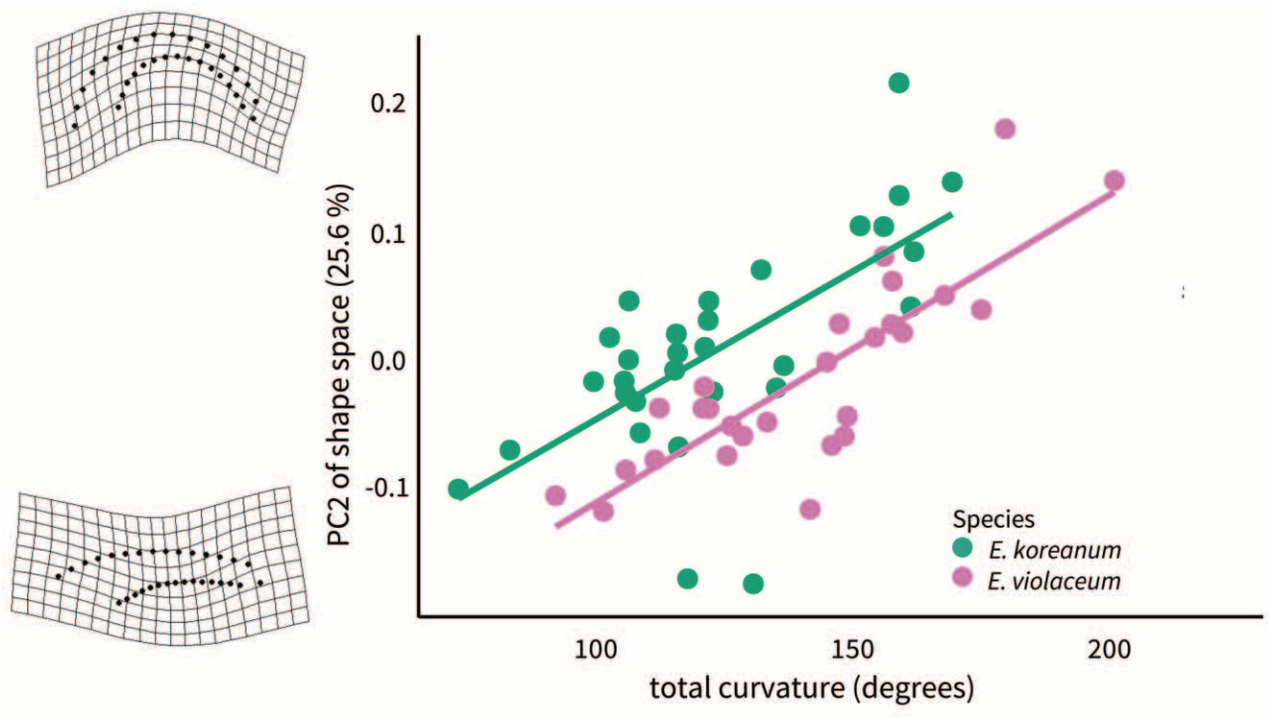

Figure 2: Scatterplot of total curvature and PC2 from a principal component analysis of geometric morphometric shape data (see also fig. S3). Curvature (which is a part of overall shape) loads strongly onto PC2, which represents the axis of second greatest variation in shape during *Epimedium* flower development. Having a landmark-based measure of curvature potentially allows this character to be partitioned from multivariate shape space.

choice because it allows us to move along the curve at uniform increments, which we denote as Δs. This proves useful when taking repeated, equally spaced measurements (such as curvature) along a curve.

As we are interested in the derivative properties of our arc-length parameterized curve, we can differentiate $\mathbf{r}(s)$ with respect to arc length s in the following way (using the formal definition of the derivative):

$$\lim_{\Delta s \to 0} \frac{\Delta \mathbf{r}(s)}{\Delta s} = \frac{d\mathbf{r}(s)}{ds} = \mathbf{T}(s).$$

This produces a tangent function $\mathbf{T}(s) = d\mathbf{r}/ds$, giving the first derivative of the parametric equation $\mathbf{r}(s)$. The tangent $\mathbf{T}(s_i)$, represented by the shorthand $\mathbf{T}_i$, contains information about the direction of the curve at position $\mathbf{r}_i$ that we can use to calculate curvature. When the tangent $\mathbf{T}$ is placed into a Cartesian plane, we can reparameterize by the angle ϕ formed with the x-axis (fig. 3). Thus, the $x'(s_i)$ and $y'(s_i)$ components of the tangent vector $\mathbf{T}_i$ can be expressed as

$$\mathbf{T}_i = \begin{bmatrix} x'(s_i) \\ y'(s_i) \end{bmatrix} = \begin{bmatrix} \cos(\phi_i) \\ \sin(\phi_i) \end{bmatrix},$$

where

$$\tan(\phi_i) = \frac{y'(s_i)}{x'(s_i)}$$

and

$$\phi_i = \arctan \frac{y'(s_i)}{x'(s_i)}.$$

At the beginning of this section we defined curvature, κ, as the rate at which the tangent is changing direction. Thus, curvature κ can be expressed as the change in the angle ϕ formed between the tangent $\mathbf{T}$ and the x-axis:

$$\kappa = \frac{d\phi}{ds}.$$

This definition provides an intuitive unit of measurement for reporting curvature: degrees of rotation per unit arc length. For example, if curvature has been calculated at every millimeter along the length of an arc, we would report its curvature as degrees per millimeter. Framed this way, curvature is a measure of rotation per unit distance. In contrast to previous definitions, where curvature is an indivisible, single property of an entire shape, here curvature is a property of every measured point along the curve. Under

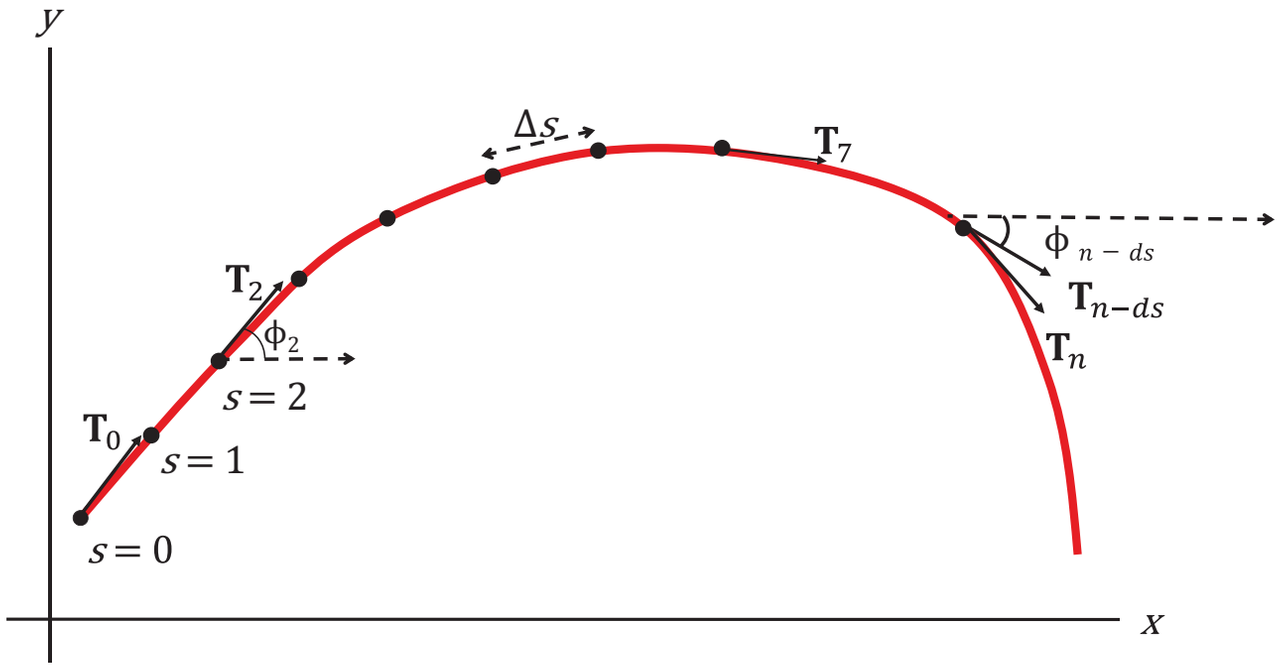

Figure 3: A curve parameterized by arc length, s. $\mathbf{T}_0$, $\mathbf{T}_2$, and $\mathbf{T}_7$ are the tangents ($d\mathbf{r}/ds$) at $s = 0, s = 2$, and $s = 7$, respectively. For convenience, the tangents are displayed as indications only, not exact representations. ϕ_2 and ϕ_{n-ds} represent the angles formed between the tangent $\mathbf{T}_2$ and the x-axis and between $\mathbf{T}_{n-ds}$ and the x-axis, respectively. Total curvature is the sum of the changes in rotation ($\Delta\phi$) along the curve.

this pointwise definition, we can summarize the total curvature (Milnor 1954) of a specimen as the total pointwise individual curvature along the curve:

$$\kappa_{\text{total}} = \int_0^{s_{\max}} \kappa \, ds.$$

Units for total curvature are no longer expressed as degrees per millimeter because we are not measuring curvature at a single point. Instead, we are integrating all tangent rotations along the curve, expressed simply as degrees. For two curves of the same shape (sensu Bookstein 1991), their total curvature will be equal, regardless of size. For example, compare the half-unit circle to another half-circle with $r = 2$. Although the second curve is larger, the total curvature of both is π radians. For comparative studies that need to account for size, we suggest dividing total curvature by arc length, s, so that the adjusted total curvature is

$$\kappa_{\text{adj}} = \frac{\kappa_{\text{total}}}{s}.$$

Using the example given above, the half-unit circle would have $\kappa_{\text{adj}} = \pi/\pi = 1$ rad, while the half-circle with $r = 2$ would have $\kappa_{\text{adj}} = \pi/2\pi = 1/2$ rad. Shape being equal, smaller curves will have greater adjusted total curvature. However, the use of this adjustment depends greatly on the biological context of the research question (Klingenberg 2016).

This concept of curvature has been embedded within the morphometrics literature since the 1970s. The widely applied tangent angle function ($\phi(t)$) defined by Zahn and Roskies (1972) describes complex shapes by measuring the tangent angle (ϕ) many times along a shape's perimeter. The resultant tangent angle graph is a unique single-valued function describing the specimen's shape and implicitly contains information about pointwise curvature (MacLeod 2011). However, because this technique was developed for quantifying shape, its utility as a curvature metric has generally not been recognized or applied (but see Van Otterloo 1991; Peterson 1993). This point is discussed further in the following section.

A Proposed Protocol for Measuring Curvature

As illustrated in our methodology review, the current protocols for measuring flower-pollinator curvature lack conceptual unity. There are two main advantages of the curvature definition described above. First, curvature becomes a local property of the tissue or organ under study. This means that shape information is gathered at every point along the curve and can be examined and compared with

other points within or between specimens. This differs from previous methods that take curvature as an indivisible property of the entire specimen. Second, because the revised definition comes directly from the field of differential geometry, we benefit from established, well-defined concepts that make clear what is meant by "curvature." When the definition of curvature is concordant between these research areas, future advances in geometry can be more readily incorporated into morphological studies.

To apply the pointwise definition of curvature, a biological organ or tissue needs to be reduced to a continuous function. To do this, we propose a protocol as illustrated in figure 4. First, a specimen is landmarked at several locations along the region of study. Second, a mathematical function is fitted to the landmarks, and finally curvature is calculated pointwise along the curve. As in all GM analyses, landmarking requires some standardization of digital photographs; this means that a unit reference (e.g., a ruler) and consistency in the angle of photography is needed (for complete guidelines, see Fruciano 2016; Savriama 2018). We note that compared with previous curvature methods, inclement weather will present a challenge if standardized photographs are to be taken in the field.

As mentioned in the previous section, the field of plant physiology was an early adopter of the pointwise definition of curvature. In one case we found curvature (as defined above) computed from cubic functions fitted to cucumber seedlings that had been landmarked by hand (Cosgrove 1990). Our protocol can be seen as a computerized version of this procedure. In another study, the total curvature of *Anthurium* Schott (Araceae) spadices was computed from fitted B-spline curves (Pour et al. 2018). However, because landmarks were not defined and the scripts are not publicly available, the reproducibility of this protocol is low. Here, we propose to develop the analysis of curvature specifically within the R programming environment (R Core Team 2017), where existing landmarking and curve-fitting procedures can be used and where modern morphometrics is being most actively developed (e.g., Adams and Otárola-Castillo 2013; Bonhomme et al. 2014).

The long-term goal of this proposal is to integrate the analysis of curvature with existing morphometrics protocols. In the following demonstration we use existing morphometric tools for landmarking and curve fitting—these were previously developed in the field of traditional and outline morphometrics (e.g., Rohlf 1990; MacLeod and

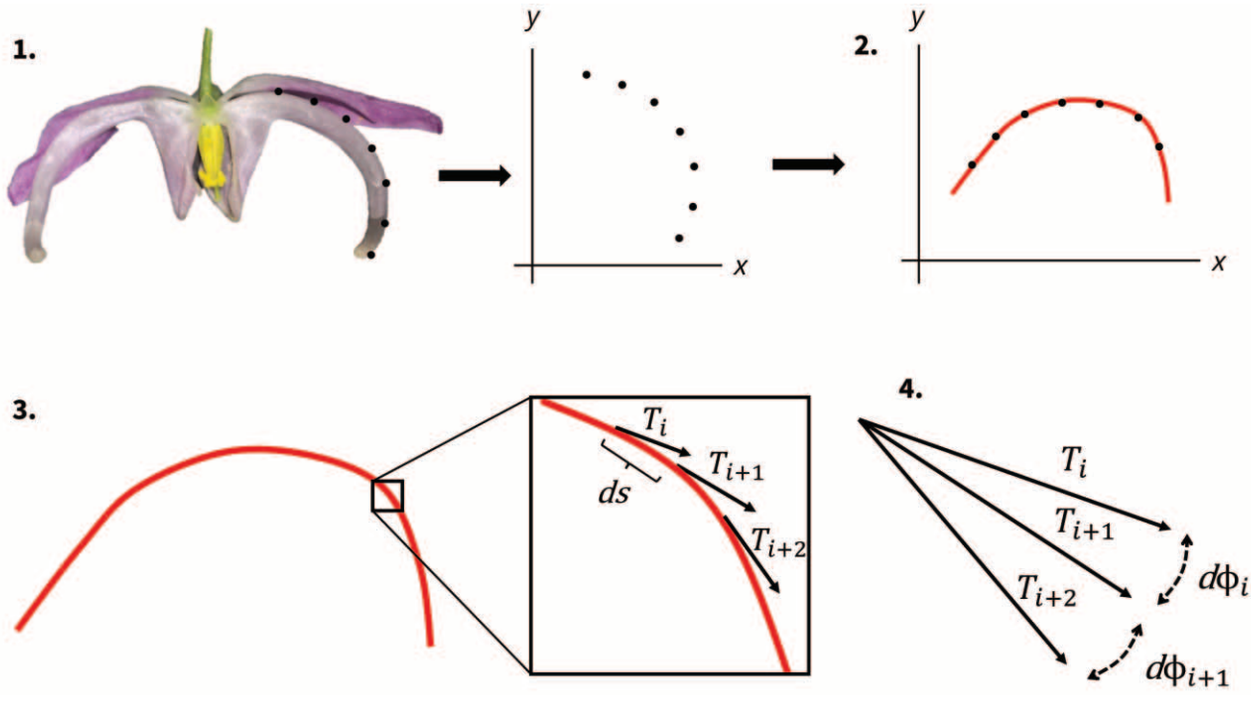

Figure 4: Proposed protocol for measuring curvature: (1) a specimen (in this case, *Epimedium violaceum*) is landmarked, semilandmarked, and assigned *xy*-coordinates within a Cartesian plane; (2) the *xy*-coordinates are rotated so that a single-valued function can be fitted to the landmarks (this step is not necessary for all cases); (3) the tangent vector **T** is calculated at an arbitrarily large number of increments, *ds*, along the curve; and (4) curvature is calculated as the rate of change of the tangent angle (ϕ) pointwise along the curve. Total curvature is calculated by the methods outlined in the section "Curvature: Concepts from Differential Geometry."

Rose 1993; Terral et al. 2004). We opted to calculate curvature from interpolating cubic splines (Perperoglou et al. 2019) fitted to landmarks. Generally, splines are suitable for accurately modeling open curves, but we encourage the development of algorithms that will compute curvature from more sophisticated curve-fitting strategies (reviewed in Rohlf 1990; MacLeod 2002). Already there is potential for existing GM algorithms to be modified to compute curvature. Notably, the tangent angle function, $\phi(t)$, describes the angle of the tangent at a landmark as a function of distance traveled along the specimen's outline (see the previous section). While the concept of ϕ (sensu Zahn and Roskies 1972) is equivalent to the one described in the previous section, the tangent angle function appears to have been derived without reference to differential geometry (Raudseps 1965). Although we are interested specifically in the curvature of shapes, the tangent angle function was developed as a means to quantify shapes in their entirety—curvature is incidental. Nonetheless, when many interpolated semilandmarks are used to model a specimen's outline (e.g., Zahn and Roskies 1972), the tangent angles could be summed to give an approximation of κ_{total}. There is great opportunity for existing tangent angle algorithms (e.g., Claude 2008) to parse curvature data as a part of an outline morphometrics analysis.

Demonstration: A Study of the Development of Curvature in *Epimedium*

Study System and Methods

In this section, we focus on the tools and protocols used to measure curvature (as defined above) in a practical demonstration. Further information on the study system and methods can be found in the supplemental PDF (available online), and all data and code have been deposited in the Dryad Digital Repository (https://doi.org/10.5061/dryad.g1jwstqrr; Boehm 2021).

We characterized the development of floral curvature in two subspecies from the *Epimedium grandiflorum* complex (Stearn 2002, pp. 140–142): *Epimedium koreanum* Nakai (*Epimedium grandiflorum* var. *koreanum* (Nakai) K.Suzuki) and *E. violaceum* C.Morren & Decne. (*Epimedium grandiflorum* f. *violaceum* (C.Morren & Decne.) Stearn). Although closely related, these taxa have notable differences in floral pigmentation and size (Stearn 2002). We investigated whether there were consequent differences in floral shape, including curvature of the prominent nectar spurs. To do this, we implement a protocol (see the previous section) largely within the R programming environment. This study serves to demonstrate that (1) the analysis of curvature can be improved by clearly defined protocols and units of measurement, (2) patterns of shape variation revealed by GM analyses can be further dissected using traditional morphometrics, and (3) measuring pointwise curvature improves estimates of total curvature for shapes not well fitted by a circle.

Following an initial description of *Epimedium* development (table S3), a set of nectar spurs ($n = 57$; table S2) of varying maturity were sampled for imaging. Spurs were photographed with a millimeter-scale reference in the dorsiventral view using a stereo microscope at a magnification of ×6.3. Digital images were imported into tpsUtil (ver. 1.76) and tpsDig (ver. 2.31; Rohlf 2015), and the dorsal and ventral arcs were each assigned 16 and 15 landmarks, respectively (supplemental PDF). The .tps files containing the landmark *xy*-coordinates were imported into R (ver. 4.0.2) using the readmulti.tps() function from geomorph (ver. 3.3.1; Adams and Otárola-Castillo 2013). Landmark configurations (shapes) were aligned using a generalized Procrustes analysis, as implemented in the geomorph::gpagen() function. Aligned shapes were then analyzed for the principal components of shape variation, using geomorph::plotTangentSpace().

The deformation grids illustrating variation in PCA shape space suggested that dorsal curvature increased along both PC1 and PC2 (fig. S3). To analyze dorsal curvature specifically, we first subset the morphometric data to include only the landmarks on the dorsal side of the nectar spurs; note that adapting (closed) landmark data for curvature analysis will vary for each study. Second, we used coo_alignxax() in Momocs (ver. 1.3.0; Bonhomme et al. 2014) to rotate each set of landmarks so that the chord was parallel to the *x*-axis. We then used the curvature_spline() function in curvr (ver. 0.0.1; Boehm 2021) to fit an interpolating cubic spline (Perperoglou et al. 2019) for each set of landmarks and compute total curvature as described in the previous section. Point curvature (K_i) was also estimated at each of the 16 landmarks per specimen. Total curvature estimates were regressed against PC2 of shape space using a linear mixed effects model (supplemental PDF).

Finally, we remeasured curvature using metrics 2–5 as outlined in the previous section. Linear measurements (e.g., chord length) were made using Momocs::coo_scalars(). Angle of declension was estimated as the angle between (1) the base of the spur and its midpoint and (2) the base of the spur and its apex (fig. S4). The inverse radius was computed from fitted circles using circlefit() in pracma (ver. 2.3.3; Borchers 2021). This function also computes the root mean square error for each fitted circle (hereafter, "circle fit"). Each inverse radius measure was multiplied by arc length to adjust for size. We then performed a pairwise regression for each metric, including the pointwise definition proposed here. At each of the 16 landmarks, we compared the inverse radius and pointwise (K_i) estimates of curvature and calculated the root mean square error per specimen (hereafter,

"pointwise error"; fig. S9). We fit a linear mixed model to the circle fit and pointwise error data. All linear models and associated tests are described in the supplemental PDF.

Results

Inspection of the deformation grids associated with PC1 and PC2 suggests that curvature is associated with both axes of shape space (fig. S3). Indeed, an explicit analysis of total curvature found a significant correlation between curvature and PC1 ($P = 3.93 \times 10^{-5}, t_{52} = 4.272, \eta_p^2 = 0.28$) and PC2 ($P = 1.86 \times 10^{-6}, t_{53} = 5.36, \eta_p^2 = 0.53$; fig. 2). Both species have comparable total curvature as their flowers emerge from bud. However, at anthesis the nectar spurs of *E. violaceum* have on average 44.2 degrees more total curvature ($P = .007, t_{49} = 3.84$; table S6; fig. S5). Inspection of pointwise curvature estimates (fig. S9) suggest that increased total curvature in *E. violaceum* is driven by the sharply curved nectar well at the apex of the spur (fig. S4).

Pairwise comparisons of the various curvature metrics found that for both species all metrics are significantly correlated ($P < 3.89 \times 10^{-7}$, Spearman's $|\rho| > 0.78$; fig. 5; tables S7, S8). However, methods 2–5 are 11% more correlated than with the total curvature metric ($P < .0001$, $t_{18} = 6.4$). We also found that specimens approximated poorly by circles are less likely to predict point curvature along the 16 landmarks ($P = .0007, t_{55} = 3.58, \eta_p^2 = 0.19$; fig. S6).

Discussion and Future Applications

The proposed definition for curvature (as adopted from differential geometry) clarifies both the concept and the units of measurement. Using the terms "pointwise curvature" and "total curvature" enables us to distinguish between the curvature at a point and the cumulative curvature of the specimen. Using this framework allowed us to examine the development of floral curvature in *Epimedium* with units of measurement (degrees) that are rooted in geometry and have a clear biological basis. This framework also considers allometry. Here we asked, Does floral curvature vary between life stages, regardless of covariation between arc length and age? Thus, we used K_{tot} instead of K_{adj}. Alternatively, to separate the effect of arc length from age, K_{adj} would be better suited.

The majority of *Epimedium* nectar spurs were well fitted by a circle. Accordingly, methods 2–5 and total curvature are highly correlated. However, for noncircular specimens there was greater discrepancy between the inverse radius and point curvature estimates. This suggests that for complex curves a pointwise metric is more able to capture local fluctuations in curvature that deviate from

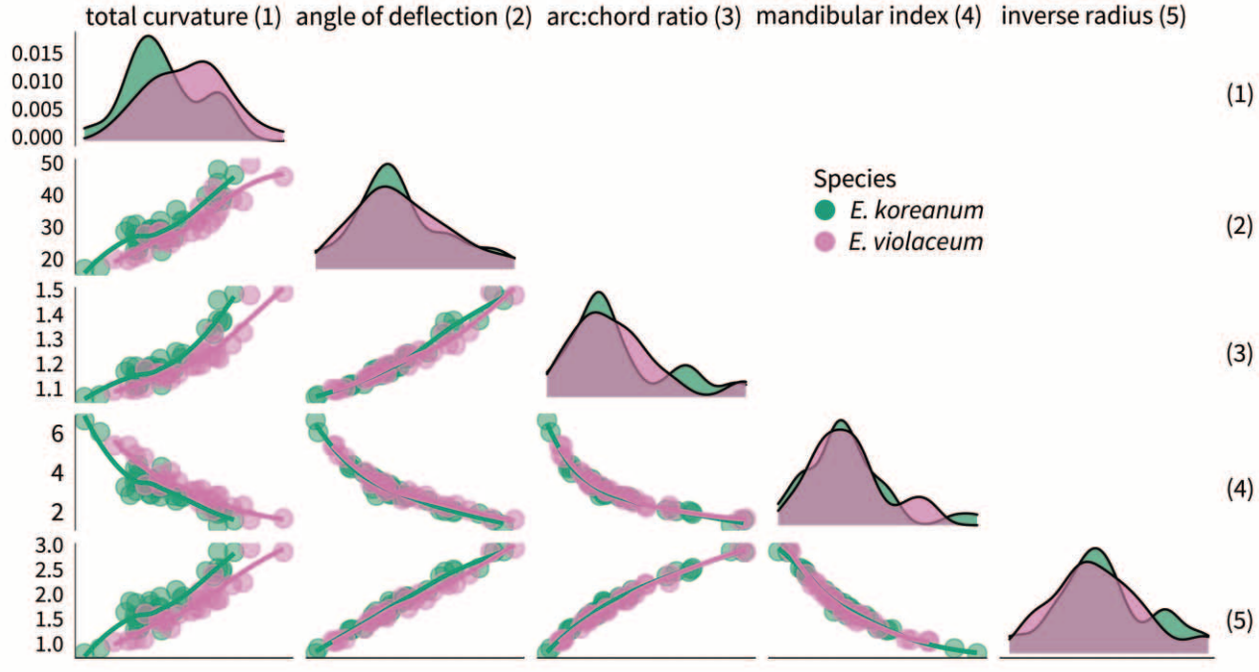

Figure 5: Pairwise comparisons of curvature metrics. Density plots show the distribution of curvature values for each species. Lines were fitted using locally estimated scatterplot smoothing (LOESS).

circularity. In this demonstration, all measurements were made from digital photographs; while this a requirement for implementing the pointwise metric, the previous metrics do not necessarily require a camera. In some contexts, the previous metrics may be more accessible and tractable when the chosen metric is known to be a good predictor of total curvature (i.e., the structure under study has constant point curvature), and local curvature features are not a focus of the study.

By pairing an analysis of curvature with GM, we are able to quantify the covariation between curvature and overall shape. Total curvature was estimated by repurposing 16 of the 31 landmarks used in the GM analysis. Thus, the comparisons with the axes of shape space are more robust than those for the previous metrics, which use at most three landmarks. Further integration of univariate metrics with GM could be achieved by modifying the PCA of shape to partial out variation due to an explanatory variable (e.g., redundancy analysis; Borcard et al. 2018). Because GM is ubiquitous among studies of biological form, we hope that this metric for curvature, as presented here, may facilitate communication via a common language between fields that are interested in curved structures. The diversity of applications spans the study of sexual selection on horn structure (e.g., in dung beetles; Emlen et al. 2005), the twining and nutation of tendrils (Bastien et al. 2014), the functional ecology of claw shape (e.g., in reptiles; Birn-Jeffery et al. 2012), the bending of hypocotyls in response to gravity and light (Silk 1989), and the biomechanics of locomotion (e.g., prehensile tails in Neotropical monkeys; Schmitt et al. 2005). Widening the applicability of this curvature metric will require drawing deeper from the morphometrics toolkit. Beyond simple curves, closed outlines might be analyzed by ZR Fourier analysis, which is well suited for decomposing a range of complex biological shapes (MacLeod 2011). As mentioned previously, the tangent angle function used to represent a closed outline mirrors the definition of curvature used in differential geometry. Fortunately, Momocs (Bonhomme et al. 2014) offers functions for ZR Fourier analysis within R, providing a convenient launch point for integrating pointwise curvature estimation with the quantification of closed outlines. With much of the groundwork already laid, estimating pointwise curvature could soon be applied to a diversity of study systems.

Conclusions

In this synthesis we discussed the ecological significance of curvature within the field of pollination ecology. In reviewing the methods used to measure curvature, we found a need for both conceptual and methodological unity. By drawing from the geometry literature, we aimed to clarify the definition of curvature within the contexts most commonly used in pollination ecology: the curvature of floral tubes or pollinator mouthparts in the dorsiventral plane. We demonstrated the utility of this revised metric by analyzing the development of curved nectar spurs in *Epimedium*. For curves that deviate from segments of circles, a pointwise definition of curvature is recommended over historical methods that model a curve as a segment of a circle. A clearly defined concept of curvature will allow integration with the broadly applied field of GM and, in pollination ecology, will facilitate a universal understanding of what is meant when we discuss curvature.

Acknowledgments

The manuscript was generously reviewed and improved by A. MacPherson, S. Otto, and two anonymous reviewers. The development of curvr was helped greatly by J. S. Légaré. S. David, J. Muñoz, and M. Scholer provided useful feedback on early versions of the manuscript. We thank D. Edgley and M. Guzman for discussions on multivariate shape data. The staff at the University of British Columbia Botanical Garden gave their expertise and kindly allowed access to the *Epimedium* plants in their collections. K. Thompson discerningly suggested the title. This work was funded by a Four Year Doctoral Fellowship (4YF) from the University of British Columbia (to M.M.A.B.) and by the Natural Sciences and Engineering Research Council (NSERC) of Canada (grants GC-2017-Q4-00199 to M.M.A.B., F18-05154 to J.E.J., and RGPIN-2019-04041 to Q.C.B.C.).

Statement of Authorship

This study was conceived and designed jointly by all of the authors. M.M.A.B. conducted the literature search, collected and analyzed the data, and drafted the first version of the manuscript. All authors contributed writing to subsequent versions of the manuscript.

Data and Code Availability

All data and scripts used in this study have been deposited in the Dryad Digital Repository (https://doi.org/10.5061/dryad.g1jwstqrr; Boehm 2021).

Literature Cited

Adams, D. C., and E. Otárola-Castillo. 2013. Geomorph: an R package for the collection and analysis of geometric morphometric shape data. Methods in Ecology and Evolution 4:393–399.

Alexandre, H., J. Vrignaud, B. Mangin, and S. Joly. 2015. Genetic architecture of pollination syndrome transition between hummingbird-specialist and generalist species in the genus *Rhytidophyllum* (Gesneriaceae). PeerJ 3:e1028.

Armbruster, W. S., and N. Muchhala. 2009. Associations between floral specialization and species diversity: cause, effect, or correlation? Evolutionary Ecology 23:159–179.

Baldwin, S. P., H. C. Oberholser, and L. G. Worley. 1931. Measurements of birds. Cleveland Museum of Natural History, Cleveland, OH.

Bardini, G., and G. M. Gianella. 2016. A historical walk along the idea of curvature, from Newton to Gauss passing from Euler. International Mathematical Forum 11:259–278.

Bastien, R., S. Douady, and B. Moulia. 2014. A unifying modeling of plant shoot gravitropism with an explicit account of the effects of growth. Frontiers in Plant Science 5:136–145.

Bell, J. 1956. Tangent, chord theorem. Mathematical Gazette 40:211–212.

Berns, C. M., and D. C. Adams. 2010. Bill shape and sexual shape dimorphism between two species of temperate hummingbirds: Black-Chinned hummingbird (*Archilochus alexandri*) and Ruby-Throated hummingbird (*Archilochus colubris*). Auk 127:626–635.

———. 2013. Becoming different but staying alike: patterns of sexual size and shape dimorphism in bills of hummingbirds. Evolutionary Biology 40:246–260.

Birn-Jeffery, A. V., C. E. Miller, D. Naish, E. J. Rayfield, and D. W. Hone. 2012. Pedal claw curvature in birds, lizards and Mesozoic dinosaurs—complicated categories and compensating for mass-specific and phylogenetic control. PLoS ONE 7:e50555.

Blüthgen, N., F. Menzel, and N. Blüthgen. 2006. Measuring specialization in species interaction networks. BMC Ecology 6:9–21.

Boehm, M. M. A. 2018. Biting the hand that feeds you: wedge-billed hummingbird is a nectar robber of a sicklebill-adapted Andean bellflower. Acta Amazonica 48:146–150.

———. 2021. curvr: an R package for measuring total curvature from landmarked specimens. R package version 0.0.1. https://github.com/mannfred/curvr.

Boehm, M. M. A., J. E. Jankowski, and Q. C. B. Cronk. Data from: Plant-pollinator specialization: origin and measurement of curvature. American Naturalist, Dryad Digital Repository, https://doi.org/10.5061/dryad.g1jwstqrr.

Bonhomme, V., S. Picq, C. Gaucherel, and J. Claude. 2014. Momocs: outline analysis using R. Journal of Statistical Software 56:1–24.

Bookstein, F. L. 1991. Morphometric tools for landmark data: geometry and biology. Cambridge University Press, Cambridge.

Borcard, D., F. Gillet, and P. Legendre. 2018. Numerical ecology with R. Springer, New York.

Borchers, H. W. 2021. Pracma: practical numerical math functions. R package version 2.3.3. http://CRAN.R-project.org/package=pracma.

Borgella, R., Jr., A. A. Snow, and T. A. Gavin. 2001. Species richness and pollen loads of hummingbirds using forest fragments in southern Costa Rica. Biotropica 33:90–109.

Bright, J. A., J. Marugán-Lobón, S. N. Cobb, and E. J. Rayfield. 2016. The shapes of bird beaks are highly controlled by nondietary factors. Proceedings of the National Academy of Sciences of the USA 113:5352–5357.

Campos, E. O., H. D. Bradshaw, and T. L. Daniel. 2015. Shape matters: corolla curvature improves nectar discovery in the hawkmoth *Manduca sexta*. Functional Ecology 29:462–468.

Cardinal, S., and B. N. Danforth. 2013. Bees diversified in the age of eudicots. Proceedings of the Royal Society B: Biological Sciences 280:20122686.

Carothers, J. H. 1982. Effects of trophic morphology and behavior on foraging rates of three Hawaiian honeycreepers. Oecologia 55:157–159.

Casey, J. 1996. Exploring curvature. Vieweg & Sohn, Braunschweig.

Castle, E. S. 1962. Phototropic curvature in *Phycomyces*. Journal of General Physiology 45:743–756.

Claude, J. 2008. Morphometrics with R. Springer Science, New York.

Collins, B. G. 2008. Nectar intake and foraging efficiency: responses of honeyeaters and hummingbirds to variations in floral environments. Auk 125:574–587.

Coolidge, J. L. 1952. The unsatisfactory story of curvature. American Mathematical Monthly 59:375–379.

Cosgrove, D. J. 1990. Rapid, bilateral changes in growth rate and curvature during gravitropism of cucumber hypocotyls: implications for mechanism of growth control. Plant, Cell and Environment 13:227–234.

Cotton, P. A. 1998. Temporal partitioning of a floral resource by territorial hummingbirds. Ibis 140:647–653.

Dakin, R., P. S. Segre, A. D. Straw, and D. L. Altshuler. 2018. Morphology, muscle capacity, skill, and maneuvering ability in hummingbirds. Science 359:653–657.

Dehling, D. M., T. Töpfer, H. M. Schaefer, P. Jordano, K. Böhning-Gaese, and M. Schleuning. 2014. Functional relationships beyond species richness patterns: trait matching in plant-bird mutualisms across scales. Global Ecology and Biogeography 23:1085–1093.

Dellinger, A. S., M. Chartier, D. Fernández-Fernández, D. S. Penneys, M. Alvear, F. Almeda, F. A. Michelangeli, et al. 2019. Beyond buzz-pollination—departures from an adaptive plateau lead to new pollination syndromes. New Phytologist 221:1136–1149.

Emlen, D. J., J. Marangelo, B. Ball, and C. W. Cunningham. 2005. Diversity in the weapons of sexual selection: horn evolution in the beetle genus *Onthophagus*. Evolution 59:1060–1084.

Feinsinger, P., and R. K. Colwell. 1978. Community organization among neotropical nectar-feeding birds. American Zoologist 18:779–795.

Fruciano, C. 2016. Measurement error in geometric morphometrics. Development, Genes and Evolution 226:139–158.

Gill, F. B., and L. L. Wolf. 1978. Comparative foraging efficiencies of some montane sunbirds in Kenya. Condor 80:391–400.

Gómez, J., F. Perfectti, J. Bosch, and J. Camacho. 2009. A geographic selection mosaic in a generalized plant-pollinator-herbivore system. Ecological Monographs 79:245–263.

Graham, C. H., J. L. Parra, C. Rahbek, and J. A. McGuire. 2009. Phylogenetic structure in tropical hummingbird communities. Proceedings of the National Academy of Sciences of the USA 106:19673–19678.

Grant, V. 1949. Pollination systems as isolating mechanisms in angiosperms. Evolution 3:82–97.

Grant, V., and K. A. Grant. 1983. Hawkmoth pollination of *Mirabilis longiflora* (Nyctaginaceae). Proceedings of the National Academy of Sciences of the USA 80:1298–1299.

Hadley, A. S., S. J. Frey, W. D. Robinson, and M. G. Betts. 2018. Forest fragmentation and loss reduce richness, availability, and specialization in tropical hummingbird communities. Biotropica 50:74–83.

Hainsworth, F. R. 1973. On the tongue of a hummingbird: its role in the rate and energetics of feeding. Comparative Biochemistry and Physiology A 46:65–78.

Hughes, M., M. Möller, T. J. Edwards, D. U. Bellstedt, and M. De Villiers. 2007. The impact of pollination syndrome and habitat

on gene flow: a comparative study of two *Streptocarpus* (Gesneriaceae) species. American Journal of Botany 94:1688–1695.

Johnson, S. D., I. Kiepiel, and A. W. Robertson. 2020. Functional consequences of flower curvature, orientation and perch position for nectar feeding by sunbirds. Biological Journal of the Linnean Society 131:822–834.

Joly, S., F. Lambert, H. Alexandre, J. Clavel, É. Léveillé-Bourret, and J. L. Clark. 2018. Greater pollination generalization is not associated with reduced constraints on corolla shape in Antillean plants. Evolution 72:244–260.

Kay, K. M., and R. D. Sargent. 2009. The role of animal pollination in plant speciation: integrating ecology, geography, and genetics. Annual Review of Ecology, Evolution, and Systematics 40:637–656.

Klingenberg, C. P. 2016. Size, shape, and form: concepts of allometry in geometric morphometrics. Development Genes and Evolution 226:113–137.

Kuhl, F. P., and C. R. Giardina. 1982. Elliptic Fourier features of a closed contour. Computer Graphics and Image Processing 18: 236–258.

Lagomarsino, L. P., E. J. Forrestel, N. Muchhala, and C. C. Davis. 2017. Repeated evolution of vertebrate pollination syndromes in a recently diverged Andean plant clade. Evolution 71:1970–1985.

Lagomarsino, L. P., and N. Muchhala. 2019. A gradient of pollination specialization in three species of Bolivian *Centropogon*. American Journal of Botany 106:633–642.

Luo, Y.-L., and Q.-J. Li. 2010. Effects of light and low temperature on the reciprocal style curvature of flexistylous Alpinia species (Zingiberaceae). Acta Physiologiae Plantarum 32:1229–1234.

MacLeod, N. 1999. Generalizing and extending the eigenshape method of shape space visualization and analysis. Paleobiology 25:107–138.

———. 2002. Geometric morphometrics and geological shape-classification systems. Earth-Science Reviews 59:27–47.

———. 2011. The centre cannot hold I: ZR Fourier analysis. Palaeontological Association Newsletter 78:35–45.

———. 2012. The centre cannot hold II: elliptic Fourier analysis. Palaeontological Association Newsletter 79:29–42.

MacLeod, N., and K. D. Rose. 1993. Inferring locomotor behavior in paleogene mammals via eigenshape analysis. American Journal of Science 293:300–355.

Maglianesi, M. A., N. Blüthgen, K. Böhning-Gaese, and M. Schleuning. 2014. Morphological traits determine specialization and resource use in plant-hummingbird networks in the Neotropics. Ecology 95:3325–3334.

———. 2015*a*. Functional structure and specialization in three tropical plant-hummingbird interaction networks across an elevational gradient in Costa Rica. Ecography 38:1119–1128.

Maglianesi, M. A., K. Böhning-Gaese, and M. Schleuning. 2015*b*. Different foraging preferences of hummingbirds on artificial and natural flowers reveal mechanisms structuring plant-pollinator interactions. Journal of Animal Ecology 84:655–664.

Manning, J. C., and P. Goldblatt. 1997. The *Moegistorhynchus longirostris* (Diptera: Nemestrinidae) pollination guild: long-tubed flowers and a specialized long-proboscid fly pollination system in southern Africa. Plant Systematics and Evolution 206:51–69.

Martén-Rodríguez, S., A. Almarales-Castro, and C. B. Fenster. 2009. Evaluation of pollination syndromes in Antillean Gesneriaceae: evidence for bat, hummingbird and generalized flowers. Journal of Ecology 97:348–359.

Maruyama, P. K., J. Sonne, J. Vizentin-Bugoni, A. M. Martín González, T. B. Zanata, S. Abrahamczyk, R. Alarcón, et al. 2018. Functional diversity mediates macroecological variation in plant-hummingbird interaction networks. Global Ecology and Biogeography 27:1186–1199.

Mclntyre, G., and K. Browne. 1996. Effect of darkening the cotyledons on the growth and curvature of the sunflower hypocotyl: evidence of hydraulic signalling. Journal of Experimental Botany 47:1561–1566.

Miller, E. T., S. K. Wagner, L. J. Harmon, and R. E. Ricklefs. 2017. Radiating despite a lack of character: ecological divergence among closely related, morphologically similar honeyeaters (Aves: Meliphagidae) co-occurring in arid Australian environments. American Naturalist 189:E14–E30.

Milnor, J. 1954. On total curvatures of closed space curves. Mathematica Scandinavica 1:289–296.

Minnaar, C., M. de Jager, and B. Anderson. 2019. Intraspecific divergence in floral-tube length promotes asymmetric pollen movement and reproductive isolation. New Phytologist 1160–1170.

Mountainspring, S. 1987. Ecology, behavior, and conservation of the Maui Parrotbill. Condor 89:24–39.

Muller, A. 1995. Morphological specializations in Central European bees for the uptake of pollen from flowers with anthers hidden in narrow corolla tubes (Hymenoptera: Apoidea). Entomologia Generalis 20:43–57.

Nath, U., B. C. Crawford, R. Carpenter, and E. Coen. 2003. Genetic control of surface curvature. Science 299:1404–1407.

Navalón, G., J. Marugán-Lobón, J. A. Bright, C. R. Cooney, and E. J. Rayfield. 2020. The consequences of craniofacial integration for the adaptive radiations of Darwin's finches and Hawaiian honeycreepers. Nature Ecology and Evolution 4:270–278.

Niet, T. van der, and S. D. Johnson. 2012. Phylogenetic evidence for pollinator-driven diversification of angiosperms. Trends in Ecology and Evolution 27:353–361.

Ollerton, J. 2017. Pollinator diversity: distribution, ecological function, and conservation. Annual Review of Ecology, Evolution, and Systematics 48:353–376.

Olsen, A. M. 2017. Feeding ecology is the primary driver of beak shape diversification in waterfowl. Functional Ecology 31:1985–1995.

Partida-Lara, R., P. L. Enriquez, J. R. Vazquez Perez, and E. Pineda Diez de Bonilla. 2018. Spatio-temporal structure of the taxonomic and functional diversity of hummingbirds at the biosphere reserve El Triunfo, Chiapas, Mexico. Ornitologia Neotropical 29:37–50.

Paton, D., and B. Collins. 1989. Bills and tongues of nectar-feeding birds: a review of morphology, function and performance, with intercontinental comparisons. Australian Journal of Ecology 14: 473–506.

Peng, F., E. O. Campos, J. G. Sullivan, N. Berry, B. B. Song, T. L. Daniel, and H. Bradshaw Jr. 2019. Morphospace exploration reveals divergent fitness optima between plants and pollinators. PLoS ONE 14:e0213029.

Perperoglou, A., W. Sauerbrei, M. Abrahamowicz, and M. Schmid. 2019. A review of spline function procedures in R. BMC Medical Research Methodology 19:1–16.

Peterson, A. T. 1993. Adaptive geographical variation in bill shape of scrub jays (*Aphelocoma coerulescens*). American Naturalist 142:508–527.

Pour, A. S., G. Chegini, P. Zarafshan, and J. Massah. 2018. Curvature-based pattern recognition for cultivar classification

of *Anthurium* flowers. Postharvest Biology and Technology 139: 67–74.

Puga-Caballero, A., M. Arizmendi, and L. A. Sánchez-González. 2020. Phylogenetic and phenotypic filtering in hummingbirds from urban environments in Central Mexico. Evolutionary Ecology 34:525–541.

Raudseps, J. G. 1965. Some aspects of the tangent-angle vs. arc length representation of contours. Ohio State University Research Foundation, Communication. Control Systems Lab.

R Core Team. 2017. R: a language and environment for statistical computing. R Foundation for Statistical Computing. https://www.R-project.org/.

Rico-Guevara, A., and M. Araya-Salas. 2014. Bills as daggers? a test for sexually dimorphic weapons in a lekking hummingbird. Behavioral Ecology 26:21–29.

Robertson, C. 1889. Flowers and Insects. II. Botanical Gazette 14:172–178.

Rocha, D., C. Monte Bello, S. Sobol, A. Samach, and M. Dornelas. 2015. Auxin and physical constraint exerted by the perianth promote androgynophore bending in *Passiflora mucronata* L. (Passifloraceae). Plant Biology 17:639–646.

Rohlf, F. J. 1990. Fitting curves to outlines. Pages 177–188 *in* F. J. Rolhf and F. L. Bookstein, eds. Proceedings of the Michigan morphometrics workshop. University of Michigan Museum of Zoology, Ann Arbor.

———. 2015. The tps series of software. Hystrix 26:1–4.

Rohlf, F., and D. Slice. 1990. Extensions of the Procrustes method for optimal superposition of landmarks. Systematic Zoology 39:40–59.

Rutter, J. W. 2000. Geometry of curves. CRC Press, Taylor; Francis Group, Boca Raton, FL.

Savriama, Y. 2018. A step-by-step guide for geometric morphometrics of floral symmetry. Frontiers in Plant Science 9:1433.

Schmitt, D., M. D. Rose, J. E. Turnquist, and P. Lemelin. 2005. Role of the prehensile tail during ateline locomotion: experimental and osteological evidence. American Journal of Physical Anthropology 126:435–446.

Scott-Elliot, G. 1890. Ornithophilous flowers in South Africa. Annals of Botany 4:265–280.

Silk, W. K. 1989. On the curving and twining of stems. Environmental and Experimental Botany 29:95–109.

Smith, T. B., L. A. Freed, J. K. Lepson, and J. H. Carothers. 1995. Evolutionary consequences of extinctions in populations of a Hawaiian honeycreeper. Conservation Biology 9:107–113.

Snow, B. K., and D. Snow. 1972. Feeding niches of hummingbirds in a Trinidad valley. Journal of Animal Ecology 41:471–485.

Sonne, J., J. Vizentin-Bugoni, P. K. Maruyama, A. C. Araujo, E. Chávez-González, A. G. Coelho, P. A. Cotton, et al. 2020. Ecological mechanisms explaining interactions within plant-hummingbird networks: morphological matching increases towards lower latitudes. Proceedings of the Royal Society B 287:20192873.

Sonne, J., T. B. Zanata, A. M. Martín González, N. L. Cumbicus Torres, J. Fjeldså, R. K. Colwell, B. A. Tinoco, et al. 2019. The distributions of morphologically specialized hummingbirds coincide with floral trait matching across an Andean elevational gradient. Biotropica 51:205–218.

Stearn, W. T. 2002. The genus *Epimedium* and other herbacious Berberidaceae including the genus *Podophyllum*. Timber, Portland.

Stein, B. A. 1987. Systematics and evolution of *Centropogon* subg. *Centropogon* (Campanulaceae: Lobelioideae). PhD diss. Washington University, St. Louis, MO.

Stiles, F. G. 1975. Ecology, flowering phenology, and hummingbird pollination of some Costa Rican *Heliconia* species. Ecology 56:285–301.

———. 1995. Behavioral, ecological and morphological correlates of foraging for arthropods by the hummingbirds of a tropical wet forest. Condor 97:853–878.

———. 2004. Phylogenetic constraints upon morphological and ecological adaptation in hummingbirds (Trochilidae): why are there no hermits in the paramo. Ornitologia Neotropical 15:191–198.

———. 2008. Ecomorphology and phylogeny of hummingbirds: divergence and convergence in adaptations to high elevations. Ornitologia Neotropical 19:511–519.

Temeles, E. J. 1996. A new dimension to hummingbird-flower relationships. Oecologia 105:517–523.

Temeles, E. J., R. S. Goldman, and A. U. Kudla. 2005. Foraging and territory economics of sexually dimorphic Purple-Throated Caribs (*Eulampis jugularis*) on three *Heliconia* morphs. Auk 122:187–204.

Temeles, E. J., C. R. Koulouris, S. E. Sander, and W. J. Kress. 2009. Effect of flower shape and size on foraging performance and trade-offs in a tropical hummingbird. Ecology 90:1147–1161.

Temeles, E. J., and W. J. Kress. 2003. Adaptation in a plant-hummingbird association. Science 300:630–633.

Temeles, E. J., J. Liang, M. C. Levy, and Y. Fan. 2019. Floral isolation and pollination in two hummingbird-pollinated plants: the roles of exploitation barriers and pollinator competition. Evolutionary Ecology 33:481–497.

Temeles, E. J., J. S. Miller, and J. L. Rifkin. 2010. Evolution of sexual dimorphism in bill size and shape of hermit hummingbirds (Phaethornithinae): a role for ecological causation. Philosophical Transactions of the Royal Society B 365:1053–1063.

Temeles, E. J., I. L. Pan, J. L. Brennan, and J. N. Horwitt. 2000. Evidence for ecological causation of sexual dimorphism in a hummingbird. Science 289:441–443.

Terral, J.-F., N. Alonso, R. B. Capdevila, N. Chatti, L. Fabre, G. Fiorentino, P. Marinval, et al. 2004. Historical biogeography of olive domestication (*Olea europaea* L.) as revealed by geometrical morphometry applied to biological and archaeological material. Journal of Biogeography 31:63–77.

Travers, S. E., E. J. Temeles, and I. Pan. 2003. The relationship between nectar spur curvature in jewelweed (*Impatiens capensis*) and pollen removal by hummingbird pollinators. Canadian Journal of Botany 81:164–170.

Tripp, E. A., and L. A. McDade. 2013. Time-calibrated phylogenies of hummingbirds and hummingbird-pollinated plants reject a hypothesis of diffuse co-evolution. Journal of Systematic and Evolutionary Botany 31:89–103.

Vamosi, J. C., S. Magallón, I. Mayrose, S. P. Otto, and H. Sauquet. 2018. Macroevolutionary patterns of flowering plant speciation and extinction. Annual Review of Plant Biology 69:685–706.

Van Otterloo, P. J. 1991. A contour-oriented approach to shape analysis. Prentice Hall, New York.

Wang, Q., Y. Li, X. Pu, L. Zhu, Z. Tang, and Q. Liu. 2013. Pollinators and nectar robbers cause directional selection for large spur circle in *Impatiens oxyanthera* (Balsaminaceae). Plant Systematics and Evolution 299:1263–1274.

Webster, M., and H. D. Sheets. 2010. A practical introduction to landmark-based geometric morphometrics. Paleontological Society Papers 16:163–188.

Weinstein, B. G., and C. H. Graham. 2017. Persistent bill and corolla matching despite shifting temporal resources in tropical hummingbird-plant interactions. Ecology Letters 20:326–335.

Young, H. J. 2008. Selection on spur shape in *Impatiens capensis*. Oecologia 156:535–543.

Zahn, C. T., and R. Z. Roskies. 1972. Fourier descriptors for plane closed curves. IEEE Transactions on Computers 100:269–281.

Zwillinger, D. 2018. Pages 424–425 *in* CRC standard mathematical tables and formulae. 33rd ed. CRC Press, Boca Raton, FL.

References Cited Only in the Online Enhancements

Berger, B. A., V. A. Ricigliano, Y. Savriama, A. Lim, V. Thompson, and D. G. Howarth. 2017. Geometric morphometrics reveals shifts in flower shape symmetry and size following gene knockdown of *CYCLOIDEA* and *ANTHOCYANIDIN SYNTHASE*. BMC Plant Biology 17:205–214.

Bodenhofer, U., E. Bonatesta, C. Horejš-Kainrath, and S. Hochreiter. 2015. Msa: an R package for multiple sequence alignment. Bioinformatics 31:3997–3999.

Buttrose, M., W. Grant, and J. Lott. 1977. Reversible curvature of style branches of *Hibiscus trionum* L., a pollination mechanism. Australian Journal of Botany 25:567–570.

Collyer, M. L., and D. C. Adams. 2018. RRPP: an R package for fitting linear models to high-dimensional data using residual randomization. Methods in Ecology and Evolution 9:1772–1779.

Dalayap, R. M., M. A. J. Torres, and C. G. Demayo. 2011. Landmark and outline methods in describing petal, sepal and labellum shapes of the flower of mokara orchid varieties. International Journal of Agriculture and Biology 13:652–658.

Hamilton, R. B. 1975. Comparative behavior of the American Avocet and the Black-necked Stilt (Recurvirostridae). Ornithological Monographs no. 17. American Ornithological Society, Chicago.

Harrell, F. E., Jr. 2020. Hmisc: Harrell miscellaneous. R package version 4.4-2. https://CRAN.Rproject.org/package=Hmisc.

Kawabata, S., M. Yokoo, and K. Nii. 2009. Quantitative analysis of corolla shapes and petal contours in single-flower cultivars of *Lisianthus*. Scientia Horticulturae 121:206–212.

Kuznetsova, A., P. B. Brockhoff, and R. H. B. Christensen. 2017. lmerTest package: tests in linear mixed effects models. Journal of Statistical Software 82:1–26.

Lenth, R., H. Singmann, and J. Love. 2018. Emmeans: estimated marginal means, aka least-squares means. R package version 1.5.3. https://CRAN.R-project.org/package=emmeans.

Lindqvist, C., T. J. Motley, J. J. Jeffrey, and V. A. Albert. 2003. Cladogenesis and reticulation in the Hawaiian endemic mints (Lamiaceae). Cladistics 19:480–495.

Nii, K., and S. Kawabata. 2011. Assessment of the association between the three-dimensional shape of the corolla and two-dimensional shapes of petals using Fourier descriptors and principal component analysis in *Eustoma grandiflorum*. Journal of the Japanese Society for Horticultural Science 80:200–205.

Ortiz, P., M. Arista, and S. Talavera. 2000. Pollination and breeding system of *Putoria calabrica* (Rubiaceae), a Mediterranean dwarf shrub. Plant Biology 2:325–330.

Preibisch, S., S. Saalfeld, and P. Tomancak. 2009. Globally optimal stitching of tiled 3D microscopic image acquisitions. Bioinformatics 25:1463–1465.

Ruan, C., H. Li, and S. Mopper. 2008. The impact of pollen tube growth on stigma lobe curvature in *Kosteletzkya virginica*: the best of both worlds. South African Journal of Botany 74:65–70.

Rueden, C. T., J. Schindelin, M. C. Hiner, B. E. DeZonia, A. E. Walter, E. T. Arena, and K. W. Eliceiri. 2017. ImageJ2: ImageJ for the next generation of scientific image data. BMC Bioinformatics 18:529–555.

Song, X., K. Gao, G. Fan, X. Zhao, Z. Liu, and S. Dai. 2018. Quantitative classification of the morphological traits of ray florets in large-flowered chrysanthemum. HortScience 53:1258–1265.

Suzuki, K. 1984. Pollination system and its significance on isolation and hybridization in Japanese *Epimedium* (Berberidaceae). Journal of Plant Research 97:381–396.

Wickham, H., M. Averick, J. Bryan, W. Chang, L. D. McGowan, R. François, G. Grolemund, et al. 2019. Welcome to the tidyverse. Journal of Open Source Software 4:1686.

Associate Editor: Marjorie G. Weber
Editor: Erol Akçay